

Adsorption Equilibrium and Kinetics Studies of Congo Red Dye Using Groundnut Shell and Sorghum Husk Biosorbent

Abubakar M. Hammari^{1,2*}, Muhammad I. Misau¹, Umar O. Aroke¹, Usman D. Hamza¹ and Abdulkarim A. Yusuf¹

¹Department of Chemical Engineering, Abubakar Tafawa Balewa University, Bauchi, Nigeria.

² Department of Biochemistry, Gombe State University, Gombe, Nigeria.

*Corresponding author:

Abubakar M. Hammari

Department of Chemical Engineering,
Abubakar Tafawa Balewa University,

Bauchi,

Nigeria.

Email: abhammari15@gmail.com

HISTORY

Received: 12th Jan 2021
Received in revised form: 15th March 2021
Accepted: 15th April 2021

KEYWORDS

Congo Red
biosorption
groundnut shell
sorghum husk
Freundlich

ABSTRACT

Groundnut Shell (GS) and Sorghum Husk (SH) were utilised as adsorbents for the adsorption of Congo Red dye. The adsorbent underwent proximate analysis and was characterised using Fourier transform infrared spectroscopy (FTIR). The effects of several experimental conditions on the adsorption extent were studied, including initial dye concentration and contact time. Spectrophotometry was used to determine the dye concentration. The equilibrium data was represented using the Langmuir, Freundlich, Temkin and Harkins, and Jura models. The Freundlich model represented the equilibrium data for Congo Red with GS better than SH. The maximal adsorption capacity of GS was determined to be 4.3660 mg/g, while SH was less efficient. The pseudo-first and pseudo-second-order kinetic equations, power function, and Elovich models were used to model adsorption data. The pseudo-second-order kinetic equation was found to best represent the sorption kinetics for all adsorption processes, as q_e experimental and q_e theoretical are nearly identical.

INTRODUCTION

Even in low quantities, the majority of the dyes have carcinogenic and molecular effects on people and aquatic life because of the existence and involvement of dangerous compounds in treatment. The major drawbacks of other processes such as ion exchange, flocculation, and solvency extraction include wasting disposal, low sensibilities, and incomplete dyes removal, the high cost of operation and capital, large energy requirements and the use of numerous reagents. Dye adsorption from such wastewater is one of the major solutions to environmental issues [1–8].

Congo Red is a derivative of carcinogenic compounds for benzidine and naphthoic acid and metabolises to carcinogenic products leading to problems, can impair and cause drowsiness and respiratory issues [9–14]. Adsorption is one of the removal methods which gets rising interest because of its potential efficiency, low power consumption, excellent molecular selectivity, easy operation and capacity to separate numerous chemical components. Certain types of contaminants are low in the sorption capacity of natural agriculture by-products. Hence, agricultural by-products are treated chemically to improve their

sorption capacity and are therefore beneficial in wastewater treatment [15–25].

MATERIALS AND METHOD

Adsorbent Collection and Preparation

The raw groundnut shell and sorghum husk were collected in Gombe town, Gombe State, Nigeria. This agricultural waste was washed thoroughly with water to remove sand, dirt and other impurities present in it and then dried in an oven at 55 °C for 24 h until all moisture contents were removed. It was then ground in a mill and sieved in a sieve shaker of particle size 80 µm. The raw groundnut shell and sorghum husk powder that passed through the sieve were stored in an airtight container and used as adsorbent without any further pre-treatment.

Preparation of Adsorbate Solutions

Analytical grade Congo Red (CR) dyes were obtained from a Biochemistry laboratory, Gombe State University. A stock solution of the dye of concentration 1000mg/l was prepared by dissolving 1 g of powdered dye in 1 L of distilled water. An experimental dye solution of desired concentration was obtained by appropriate dilution of the stock solution.

Adsorbent Characterization

Fourier transform infra-red (FTIR) spectrophotometer was used to identify the different functional groups available on the adsorbent sites. The FTIR of the adsorbent will be taken before adsorption using FTIR spectrophotometer. 0.1 g of each adsorbent will be encapsulated with 1 g of KBr spectroscopy grade and by introducing the mix in a piston's cell of a hydraulic pump with compression pressure 15 KPa/cm²; the solid translucent disk will be obtained which will introduce in an oven for 4 h at 105 °C to ensure the non-interference of any existing water vapours or CO₂ molecules. The FTIR spectrum will then be recorded within the wavenumber range 4000 – 450 cm⁻¹ [26].

Proximate Analysis

The proximate analysis determines the moisture content, volatile matter content, ash content, and fixed carbon. The first three were determined in the laboratory and the fixed carbon was calculated by difference.

Determination of Moisture

Moisture can be removed by air-drying but the inherent moisture can only be removed completely by drying in an oven at 105°C for about an hour. The added amount of free and inherent moisture is called total moisture. 250 mL beakers are cleaned and dried. The weight of the beaker is taken, and one gram of each sample is weighed in the beaker (W1). Then it is heated in an electric oven out of contact with air (to avoid oxidation) at 105°C temperature for an hour. After heating, the beaker was transferred to a desiccator and rapidly reweighed (W2). The difference in weight (i.e., W1 - W2) gave the amount of moisture. Moisture content is expressed in percentage.

Determination of ash content

The residue left after burning is known as ash. It is generally composed of inorganic substances. 1 gm of powdered GS and SH is weighed in a crucible (W1). Then the crucible is kept inside a muffle furnace and the temperature is gradually raised to 800 °C. At 800 °C the temperature is kept constant, and the incineration of the sample is completed by heating for an hour at that temperature. After incineration, the crucible is allowed to cool and transferred to desiccators. Then the basin (crucible) is reweighed (W2). Deduction of W1 (weight of the basin) from W2 (weight of the basin + ash) gives the amount of ash in the sample. Ash content is expressed in percentage [27].

Determination of volatile matter

The volatile matter, sometimes called volatiles consists mainly of the gases and water and tarry vapours evolved from the sample when it is heated at high temperature. To determine it, 1 gm of sample is taken in a crucible. The weight of the silica crucible and a sample is W1. The sample is then heated for 7 minutes at a constant temperature of 925 °C inside a furnace. After heating, the crucible is cooled and transferred to desiccators. After few minutes the silica crucible is re-weighed (W2). The difference between W1 and W2 gives the amount of apparent volatile matter in the sample. The actual volatile matter is obtained after deducting the moisture content of the sample. Volatile matter content is expressed in percentage [27].

Calculation of fixed carbon (F.C.)

The fixed carbon represents the carbon content in a sample that has not been combined with any other element (in a free state). The amount of fixed carbon is computed by subtracting the sum of the percentage of moisture, volatile matter and ash from hundred.

Fixed carbon = 100 - (moisture % + ash % + volatile matter %) [27].

Phytochemical Analysis

Test for Flavonoids

2 mL of the filtered sample was dissolved in 10 % NaOH of the solution to give a yellow colour. A change of colour from yellow to colourless on the addition of dilute hydrochloric acid indicates the presence of flavonoids [28].

Test for Steroid

To a small amount of the extract, 2 mL of chloroform was added than a volume of conc. H₂SO₄ was added by sides. The turning of red in the upper layer and yellow with green fluorescence in the sulphuric acid layer indicates the presence of steroids [28].

Test for Glycoside

To 5 mL boiling distilled water, 1 g of the bark was added, stirred and then filtered through filter paper. Few drops of conc. HCl was added to a 2 mL portion of the filtrate. It was boiled for few minutes to hydrolyze any glycosides present, few drops of aqueous ammonia solution were added to make the mixture alkaline. Then three drops of the mixture were added to 2 ml of Benedict's reagent and boiled. A reddish-brown indicates the presence of glycosides [28].

Test for Saponin

1 ml of the extract was shaken with distilled water in a test tube, frothing which persists on warming indicates the presence of saponin [28].

Test for Tannins

A small quantity of the extract was mixed with distilled water and heated on a water bath. The mixture was filtered while Conc. H₂SO₄ and 5 % ferric chloride were added to the filtrate. A blue-black, green or blue-green precipitate indicates the presence of tannins [28].

Test for Alkaloids

2 mL of the extracts was stirred with 5 mL of 1 % aqueous hydrochloric acid on a water bath and filtered. Few drops of Dragendorff's solution was added to the filtrate, the presence of orange-red precipitate indicates the presence of alkaloids [28].

Batch Adsorption Experiments

Batch adsorption of CR dyes onto the adsorbent groundnut shell and Sorghum husk was conducted in a 250 mL airtight Erlenmeyer flask containing 200 mL of known concentration of the dyes solution and an accurately weighed amount of the optimum adsorbent dosage of 4 g and 3.6 g for GS and SH respectively [29]. The mixtures in the flasks were agitated on a mechanical shaker operating at a constant speed of 200 rpm. The effect of contact time (30, 60, 90, 120 and 150 min), initial dye concentration (10, 20, 30, 40 and 50 mg/L), and temperature (298, 303, 313, 323 and 333 K) was evaluated. The flask containing the samples was withdrawn from the shaker at a predetermined time interval, filtered and the final concentration of the dyes in the supernatant solutions was analyzed using the UV-visible spectrophotometer. The pH of the solution was adjusted using 1M HCl or NaOH to the optimum pH of 3.0 [29].

The amount of equilibrium uptake of the dyes was determined using:

$$q_e = \frac{(C_0 - C_e)V}{M} \quad (1)$$

$$\%Dye\ Removal = \frac{(C_0 - C_e)V}{M} \times 100 \quad (2)$$

Where q_e is the amount of dye taken up by the adsorbent at equilibrium (mg/g), C_0 is the initial dye concentration (mg/L), C_e is the dye concentration at equilibrium (mg/L), M is the mass of the adsorbent (g), and V is the volume of the solution, (L).

Equilibrium adsorption Experiment

Equilibrium adsorption experiments were conducted at average room temperature. A predetermined volume of dye solution will be added to 250 mL stoppered Erlenmeyer flasks containing an appropriate mass of Groundnut shell and Sorghum husk powder and agitated on the mechanical shaker at 200 rpm. Portions of residual dye samples were removed from the flasks periodically and filter. The absorbance of the residual dye was read at the maximum wavelength of 665 nm and scanned using a UV/visible spectrophotometer. The residual dye, q_e (mg/g), was calculated from equation 2 above.

The kinetics experiments were conducted similar to those for batch adsorption. The adsorption kinetic data was assessed using four models: Pseudo First Order, Pseudo Second Order, Elovich and Power Function Kinetics Equations as stated in Equations 3, 4, 5, 6 and 7 respectively. Kinetics equation based on the concentration of solution and adsorption capacity of solid, Lagergren’s first-order rate equation has been called pseudo-first-order. The linear form of the pseudo-first-order kinetic model [26] is represented by;

$$\ln(q_e - q_t) = \ln q_e - k_1 t \quad (3)$$

Where q_e and q_t are the values of the amount of the dye adsorbed per unit mass on the adsorbent at equilibrium and at various time t , respectively, k_1 is the Pseudo-first-order adsorption rate constant (min^{-1}). The values of k_1 and calculated q_e can be determined from the slope and intercept respectively, of the linear plot of $\ln(q_e - q_t)$ versus t .

The pseudo-second-order kinetic model [26] is expressed by;

$$\frac{t}{q_t} = \frac{1}{k_2 q_e^2} + \frac{1}{q_e} \quad (4)$$

Where k_2 is the pseudo-second-order adsorption rate constant ($\text{g/mg}\cdot\text{min}$) and q_e is the amount of dye adsorbed (mg/g) on the adsorbent at equilibrium. The initial adsorption rate, h ($\text{mg/g}\cdot\text{min}$) is expressed as:

$$h = k^2 q_e \quad (5)$$

The plot of t/q_t versus t gives a linear relationship which allows computation of k_2 , h and calculated q_e . Among these models, the criterion for their applicability is based on judgment on the respective correlation coefficient (R^2) and agreement between the experimental and calculated value of q_e , [30].

Elovich equation is also used successfully to describe second-order kinetic assuming that the actual solid surfaces are energetically heterogeneous, but the equation does not propose any definite mechanism for adsorbate-adsorbent [31]. It has extensively been accepted that the chemisorption process can be

described by this semi-empirical equation [32]. The linearized form of the Elovich kinetic equation (model) is expressed by [30].

$$q_t = \frac{\ln(\beta\alpha)}{\beta} - \frac{\ln t}{\beta} \quad (6)$$

Where: α is the initial adsorption rate ($\text{mg}\cdot\text{g}^{-1}\cdot\text{min}^{-1}$) and β is the desorption constant ($\text{mg}\cdot\text{g}^{-1}\cdot\text{min}$) if the adsorption fits the Elovich model, a plot of q_t versus $\ln(t)$ should yield a linear relationship with a slope of $(1/\beta)$ and an intercept of $(1/\beta) \ln(\beta\alpha)$.

The power function kinetic equation (model) is represented by:

$$\log q_t = \log a + b \log t \quad (7)$$

Where: the constant, a , represents the initial rate ($\text{mg}\cdot\text{g}^{-1}\cdot\text{min}^{-1}$) and the constant b represents the rate constant of the reaction ($\text{g/mg}\cdot\text{min}$). If the adsorption fits the power function model, a plot of $\log q_t$ versus $\log t$ should yield a linear relationship with a slope of b and intercept $\log a$ [33].

RESULTS AND DISCUSSION

The Brunauer Emmet Teller (BET) surface area measurement technique was used to find the characteristics of the sample. Pore volume and pore volume distribution of adsorbents play an important role in adsorption [34]. The BET surface analysis for the unmodified sorghum husk has a surface area of $139.539 \text{ m}^2/\text{g}$, pore volume of 0.053 cc/g , pore width of 2.647 nm , micropore surface area of $180.937 \text{ m}^2/\text{g}$ whereas the unmodified groundnut shell has a surface area of $302.522 \text{ m}^2/\text{g}$, pore volume of 0.091 cc/g , pore width of 2.647 nm , micropore surface area of $326.976 \text{ m}^2/\text{g}$ [29].

Fourier Transform Infra-Red (FTIR) Spectroscopy

The FTIR spectral of SH and GS powder obtained within the spectral range of $4000\text{-}450 \text{ cm}^{-1}$ as shown in **Figs. 1 and 2** respectively, displayed the characteristics peaks of the correspondent adsorbent such as prominent peak at 3477.79cm^{-1} and 3450.68 cm^{-1} for SH and GS respectively due to hydroxyl group, O-H bond, probably attributed to adsorbed water. The peaks at the region of 2925.84cm^{-1} SH and 2925.44cm^{-1} GS were attributed to C-H interaction with the surface of the adsorbent indicating the carbon dioxide of normal air. The peak at 1642.67cm^{-1} and 1633.29cm^{-1} for SH and GS respectively shows the presence of C=C bond from alkenes. The characteristics band at 1033.57cm^{-1} SH and 1032.71cm^{-1} GS corresponds to C-O bond, confirming the presence of carboxylic acid [29,35].

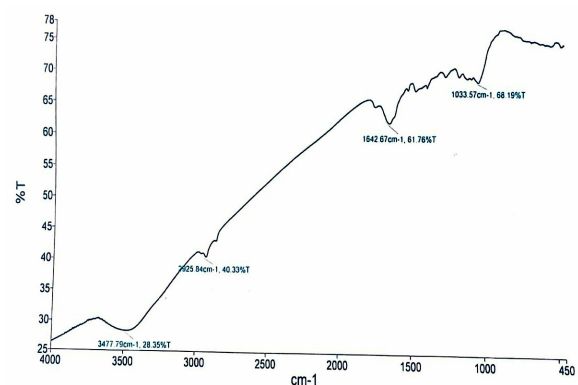


Fig. 1 FTIR Spectra of Sorghum Husk.

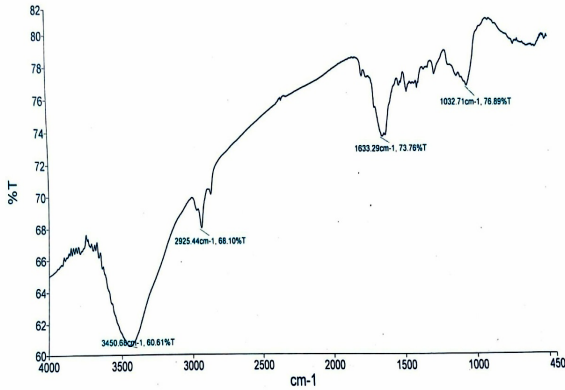


Fig. 2. FTIR Spectra of groundnut shell.

Proximate Analysis

The result of the proximate compositions of the adsorbent samples is presented in Table 3. The moisture, volatile matter, ash and fixed carbon content of the adsorbent were: 7.63, 3.124, 11.97 and 77.276%, respectively for GS and the moisture, volatile matter, ash and fixed carbon content of the adsorbent were: 7.07, 13.824, 15.85 and 63.256%, respectively for SH.

Table 3. Proximate analysis of groundnut shell and sorghum husk.

	Moisture %	Ash %	Volatile Matter %	Fixed Carbon %
Groundnut Shell	7.63	11.97	53.124	27.276
Sorghum Husk	7.07	15.85	45.824	31.256

Phytochemical Screening

The result of the phytochemical screening of the adsorbent samples is presented in Table 4. The Phytochemical analysis was done qualitatively, the plus (+) sign indicating the presence of the respective phytochemical parameter in very small amount and (+++) in large amount whereas the negative (-) sign indicating the absence of the respective Phytochemical parameter

Table 4. Phytochemical analysis of groundnut shell and sorghum husk.

Phytochemicals	Groundnut		Sorghum
	Shells	Husk	
Alkaloids	+		+++
Saponins	-		-
Tannins	-		-
Steroids	+		-
Glycosides	-		-
Flavanoids	-		-

Effect of initial dye concentration

Fig. 3 also depicts the influence of initial CR dye concentration. The % elimination of CR dye increased with increasing starting concentration in both the GS and SH. This discovery could be explained by the fact that when dye concentration increases, more dye molecules become available for adsorption by the adsorbents. This is due to the action of the concentration gradient, which is the primary driving force behind the adsorption process. Intidhar et al. observed a similar pattern [36]. Furthermore, as the initial dye concentration increased, the equilibrium adsorption capacity (q_e) of both biosorbents increased. This is because increasing dye concentration increases the driving power required to overcome all CR mass transfer resistances between the aqueous and solid phases, increasing equilibrium adsorption capacity [23,24].

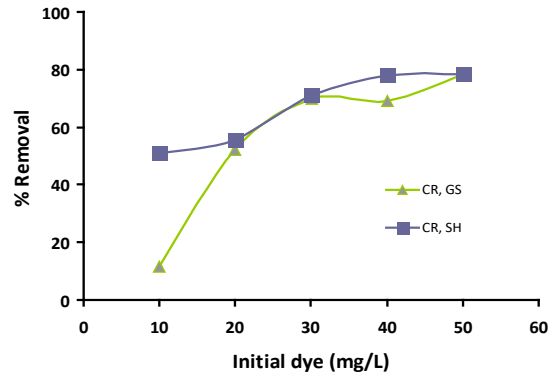


Fig. 3. Effect of initial dye concentration for congo red onto groundnut shell and sorghum husk

Effect of contact time for Congo Red

Contact time is one of the physical characteristics that is employed in the economic design of wastewater treatment plants [27]. Fig. 4 further demonstrates that the removal of CR dye from both the GS and SH solutions is quick in the beginning and that the velocity approaching the balance diminishes. Because the surface of the adsorption process is big at first, adsorption to this surface is rapid. The equilibrium period in CR dye adsorption was determined to be 60 minutes for SH and 30 minutes for GS.

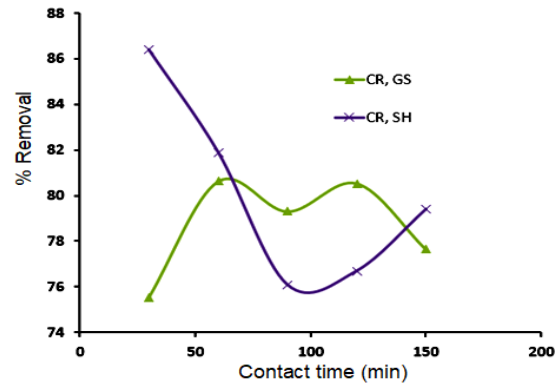


Fig. 4. Effect of contact time for Congo Red onto Groundnut Shell and Sorghum Husk

Calibration curves

The UV/VIS spectrophotometer was used to determine the concentration of CR in solution at a maximum absorption wavelength, λ_{max} . This was determined by varying the wavelength of the spectrophotometer from 400nm to 1100nm. The wavelength at which the absorbance is highest was the maximum wavelength for a particular dye. The maximum wavelength of the Spectrophotometer for the determination of the absorbance of CR was found to be 510nm. All the absorbance measurements for CR were carried out using a UV/VIS Spectrophotometer set at the maximum wavelength, λ_{max} of 510 nm.

A calibration curve was plotted between absorbance and certain concentrations of dye solution. Unknown CR concentrations were measured using the calibration curve. To obtain the standard calibration curve 5 samples of different concentrations 10, 8, 6, 4 and 2 mg/l were prepared. The absorbance of each sample was then measured at their respective

maximum wavelength. The absorbance was plotted against the concentrations to obtain a standard calibration curve.

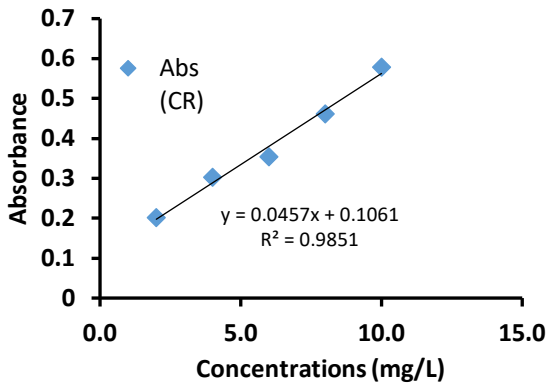


Fig. 6. Standard calibration curve.

Equilibrium isotherm models

Isotherm models

Table 5. Equilibrium isotherms parameters.

Model	Parameters	GS	SH
Langmuir	q_m (mg/g)	4.3660	-4.9188
	K_L (l/mg)	0.0651	-0.0257
	R^2	0.6689	0.5232
Freundlich	K_f	0.0039	0.0079
	n	0.8434	0.8473
	R^2	0.9033	0.9779
Temkin	KT (mol/k)	0.3941	0.4607
	B (kj/mol)	1.0674	1.1735
	R^2	0.7150	0.8910
Harkin and Jura	A	0.0011	0.0316
	B	1.0569	0.9939
	R^2	0.2738	0.4557

The Langmuir, Freundlich, Temkin and Harkins, and Jura isotherm models were used to describe the connection between the CR dye concentration in the aqueous solution and the GS and SH biosorbents. Fig. 7–10 show the plots of the various isotherms. Table 5 summarizes the intercept and slope values acquired for each plot. The experimental data fit well to both the GS and SH for Freundlich isotherm models when the linear square regression correlation coefficient, R^2 , was compared (Table 5). Furthermore, the Freundlich isotherm constant, n was found to be smaller than one, indicating that CR adsorption by GS and SH is a chemical process [33]. These findings support the Freundlich isotherm's ability to represent CR adsorption onto GS and SH powder, with adsorption occurring mostly on the heterogeneous surface of the GS and SH powder. Fig. 7 depicts the Langmuir isotherm model for the adsorption of CR onto GS and SH.

The Langmuir isotherm was found to be less suitable for the adsorption of CR by both adsorbents based on the poor correlation coefficient (R^2) values presented in Table 5. The maximal CR dye sorption capacity of GS and SH powders was determined to be 4.3688 mg/g and -4.9188 mg/g, respectively. Fig. 9 depicts the Temkin isotherm model for the adsorption of CR onto GS and SH, and Table 5 calculates and summarizes the Temkin parameters. Fig. 9 shows that the Temkin model was less suitable for CR adsorption onto GS and SH powder. The correlation coefficient (R^2) values for GS and SH were 0.72 and 0.89, respectively, indicating that the Temkin model adequately explained the adsorption of CR onto GS and SH. Furthermore, it

can be shown in Table 5 that the values of heat of adsorption, B , were determined to be (less than) 8 kJ/mol, indicating a weak interaction between the CR dye and the GS and SH powder, and therefore the process can be described as chemical adsorption [37]. The Harkin and Jura isotherms did not fit the experimental data well. Table 5 also includes the Harkin and Jura constants, A and B , as well as the correlation coefficients R^2 for CR. The curve of $1/qe^2$ against $\log C_e$ in Fig. 10 was equally nonlinear, with a low R^2 , implying that it was insufficient for modelling CR adsorption onto GS and SH powder.

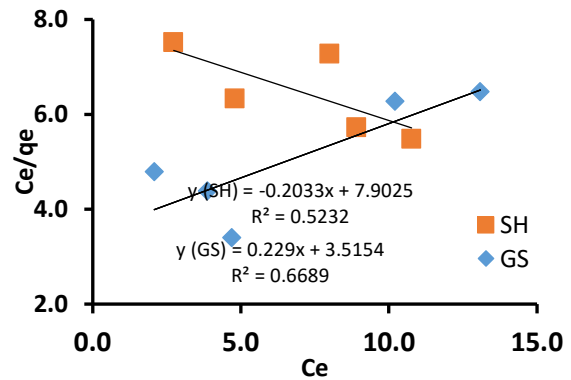


Fig. 7. Langmuir isotherm model.

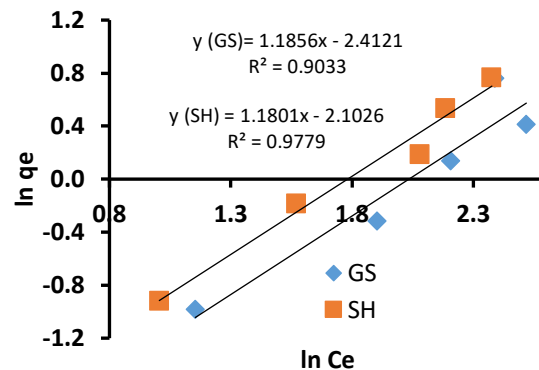


Fig. 8. Freundlich isotherm model.

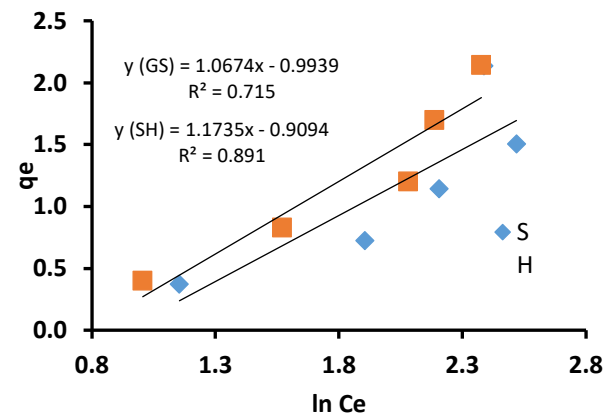


Fig. 9. Temkin isotherm model.

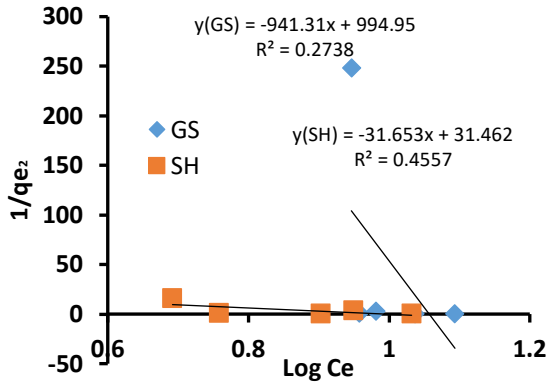


Fig. 10. Harkins and Jura Isotherm model.

Kinetic model

In this situation, kinetic data agrees better with pseudo-second-order in terms of coefficient of determination (R^2) than pseudo-first-order in both cases of adsorbents, GS and SH. **Table 6** shows the kinetic parameters of adsorption. The predicted q_e values for the pseudo-second-order model were close to the experimental values based on kinetic data. The suitability of the pseudo-second-order model implies that chemisorption is the rate-limiting step. The valence forces that exist between biosorbent and sorbate molecules help explain this chemical adsorption [31]. The Elovich model did not fit the experimental data well. **Table 6** also includes the Elovich constants, and the correlation coefficients R^2 .

The plot of q_t vs $\ln t$ in **Fig. 11** was also nonlinear, with a low R^2 , indicating that the Elovich model was insufficient for modelling the adsorption of CR onto GS and SH powder. The power function model did not also fit the experimental data well. **Table 6** shows the power function constants, a and b , as well as the correlation coefficients, R^2 . The plot of $\log q_t$ vs $\log t$ in **Fig. 14** was nonlinear and had a poor R^2 , indicating that the power function model was insufficient for modelling the adsorption of CR onto GS and SH powder.

The removal of dyes from wastewater is an issue of major environmental significance in water contamination. Methylene blue is generally the water's most soluble teal; used for cotton and tannin printing, leather dyeing, medicinal and antibacterial applications. Cationic dyes such as methylene blue are more harmful than anionic dyes such as Red Congo. Therefore, before it is released, the colours must be removed from wastewater. Due to their flexibility and high adsorption efficiency, but also because of their cost and the difficulty of regeneration, it was founded that adsorption is one of the most effective methods for the removal of dyes from wastewater, with activated carbon as the industry's most commonly used adsorber.

Phytochemical and proximate investigations described this adsorbent. Differences in initial concentration, time and temperatures were examined for MB's and CR removal efficiency. The Langmuir, Freundlich, Temkin, Harkins and Jura Isotherms data were tested for their ability to fit the data. Most of the sorption process was determined to be chemical.

Kinetic models for biosorption with generated data utilising first order, second order pseudo, Elovich and power function. The second pseudo-order has been identified as the best kinetic model (**Fig. 12**) with good R^2 values. Thermodynamic parameters such as ΔG , ΔH and ΔS have been evaluated and it has been found that most of the sorption process was spontaneous and exothermic (Data not shown).

Table 6. Kinetic models parameters.

Kinetic Model	Parameter	GS	SH
Pseudo First Order	$q_{e, cal}$ (mg/g)	0.0883	0.0449
	$q_{e, exp}$ (mg/g)	2.1670	2.0470
	K_1 (min^{-1})	0.0025	-0.0139
	R^2	0.0274	0.5817
Pseudo Second Order	h (mg/gmin)	6.5053	0.1779
	$q_{e, cal}$ (mg/g)	2.1482	1.9149
	$q_{e, exp}$ (mg/g)	2.1670	1.9170
	K_2 (g/mg min)	-1.1873	-0.2203
Elovich	R^2	0.9983	0.9971
	b	-0.187	0.1981
	a	2.2179	0.1703
	R^2	0.2437	0.7028
Power Function	a	7.4E-8	2.79E14
	b	0.0216	-0.0681
	R^2	0.2437	0.7028

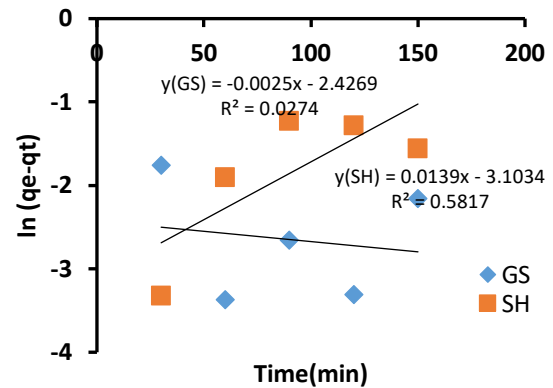


Fig. 11. Pseudo First order kinetic model for CR.

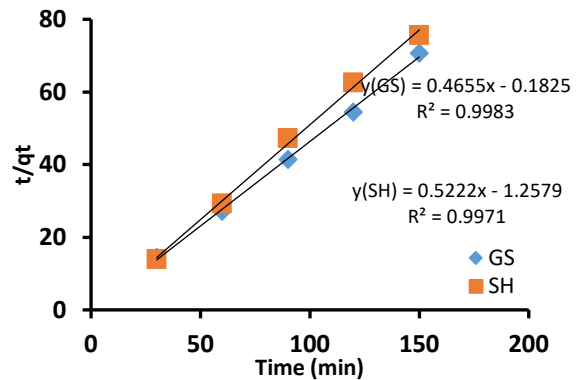


Fig. 12. Pseudo Second order kinetic model.

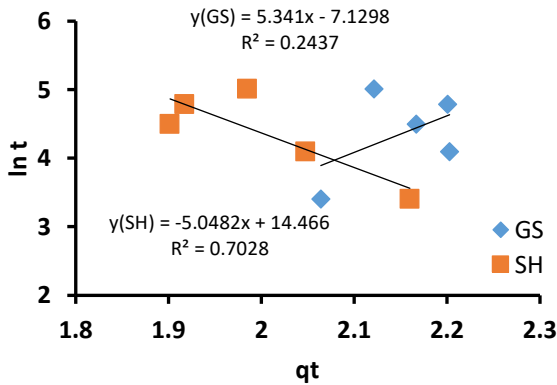


Fig. 13. Elovich kinetic model.

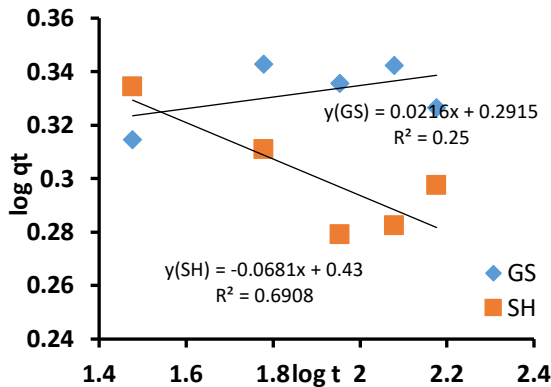


Fig. 14. Power function kinetic model for CR.

CONCLUSION

In this investigation, we have examined the application of agricultural waste to tackle the problem of dye-filled wastewater. Two bio-sourcing products were successfully employed as an adsorbent to remove Congo Red (CR) from aqueous solutions for this purpose. Various aspects such as starting concentration of colour and time influenced the adsorption. With increasing dye concentration in the process, the removal efficiency rose. For description of the adsorption balances of CR dye on GS and SH, the adsorption isothermal models Langmuir, Freundlich, Temkin and Harkin and Jura. The findings on SH were well coordinated with Freundlich isotherm, the Temkin Isotherm with all adsorbents. The easiest way to evaluate the kinetic parameters of the adsorption process was to add the dye to two adsorbents was to fit the second pseudo model.

REFERENCES

1. Aksu Z. Application of biosorption for the removal of organic pollutants: A review. *Process Biochem.* 2005;40(3–4):997–1026.
2. Aksu Z, Tezer S. Equilibrium and kinetic modelling of biosorption of Remazol black B by *Rhizopus arrhizus* in a batch system: Effect of temperature. *Process Biochem.* 2000;36(5):431–9.
3. Barka N, Abdennouri M, Makhfouk MEL. Removal of Methylene Blue and Eriochrome Black T from aqueous solutions by biosorption on *Scolymus hispanicus* L.: Kinetics, equilibrium and thermodynamics. *J Taiwan Inst Chem Eng.* 2011;42(2):320–6.
4. Santos SCR, Bacelo HAM, Boaventura RAR, Botelho CMS. Tannin-Adsorbents for Water Decontamination and

- for the Recovery of Critical Metals: Current State and Future Perspectives. *Biotechnol J.* 2019;14(12).
5. Mahamadi C. Will nano-biosorbents break the Achilles' heel of biosorption technology? *Environ Chem Lett.* 2019;17(4):1753–68.
6. Tabaraki R, Heidarzadi E. Simultaneous multidye biosorption by chemically modified *Sargassum glaucescens*: Doehlert optimization and kinetic, equilibrium, and thermodynamic study in ternary system. *Sep Sci Technol Phila.* 2017;52(4):583–95.
7. Cardoso NF, Lima EC, Calvete T, Pinto IS, Amavisca CV, Fernandes THM, et al. Application of Aqai Stalks As Biosorbents for the Removal of the Dyes Reactive Black 5 and Reactive Orange 16 from Aqueous Solution. *J Chem Eng Data.* 2011 May 12;56(5):1857–68.
8. Farah JY, El-Gendy NSh, Farahat LA. Biosorption of Astrazone Blue basic dye from an aqueous solution using dried biomass of Baker's yeast. *J Hazard Mater.* 2007;148(1–2):402–8.
9. Abbas M, Trari M. Kinetic, equilibrium and thermodynamic study on the removal of Congo Red from aqueous solutions by adsorption onto apricot stone. *Process Saf Environ Prot.* 2015;98:424–36.
10. Abu Talha M, Goswami M, Giri BS, Sharma A, Rai BN, Singh RS. Bioremediation of Congo red dye in immobilized batch and continuous packed bed bioreactor by *Brevibacillus parabravis* using coconut shell bio-char. *Bioresour Technol.* 2018 Mar 1;252:37–43.
11. An S-Y, Min S-K, Cha I-H, Choi Y-L, Cho Y-S, Kim C-H, et al. Decolorization of triphenylmethane and azo dyes by *Citrobacter* sp. *Biotechnol Lett.* 2002;24(12):1037–40.
12. Arumugam A, Saravanan M. Adsorption of congo red dye from aqueous solution onto a low-cost natural orange peel and groundnut shell powder. *Pharm Lett.* 2015;7(12):332–7.
13. Ayed L, Achour S, Khelifi E, Cheref A, Bakhrouf A. Use of active consortia of constructed ternary bacterial cultures via mixture design for Congo Red decolorization enhancement. *Chem Eng J.* 2010;162(2):495–502.
14. Bhaumik M, McCrindle R, Maity A. Efficient removal of Congo red from aqueous solutions by adsorption onto interconnected polypyrrole-polyaniline nanofibres. *Chem Eng J.* 2013;228:506–15.
15. Yang Y, Wang G, Wang B, Li Z, Jia X, Zhou Q, et al. Biosorption of Acid Black 172 and Congo Red from aqueous solution by nonviable *Penicillium YW 01*: Kinetic study, equilibrium isotherm and artificial neural network modeling. *Bioresour Technol.* 2011;102(2):828–34.
16. Pourang N, Rezaei M. Biosorption of copper from aqueous environment by three aquatics-based sorbents: A comparison of the relative effect of seven important parameters. *Bioresour Technol Rep.* 2021 Sep 1;15:100718.
17. Fathollahi A, Khasteganan N, Coupe SJ, Newman AP. A meta-analysis of metal biosorption by suspended bacteria from three phyla. *Chemosphere.* 2021 Apr 1;268:129290.
18. Blagojev N, Vasić V, Kukić D, Šćiban M, Prodanović J, Bera O. Modelling and efficiency evaluation of the continuous biosorption of Cu(II) and Cr(VI) from water by agricultural waste materials. *J Environ Manage.* 2021 Mar 1;281:111876.
19. Yahuza S, Sabo IA, Abubakar A, Shukor MY. Biosorption of Lead (II) Ions by Brown Algae: A Thermodynamic Study. *Bull Environ Sci Sustain Manag E-ISSN 2716-5353.* 2020 Dec 31;4(2):1–5.
20. Abubakar A. Test for Outlier and Normality of the Residuals for the Pseudo-1st Order Kinetic Modelling of Glyphosate Adsorption onto Palm Oil Fronds. *Bull Environ*

- Sci Sustain Manag E-ISSN 2716-5353. 2020 Dec 31;4(2):18–22.
21. Alipanah M, Park DM, Middleton A, Dong Z, Hsu-Kim H, Jiao Y, et al. Techno-Economic and Life Cycle Assessments for Sustainable Rare Earth Recovery from Coal Byproducts using Biosorption. ACS Sustain Chem Eng. 2020 Dec 14;8(49):17914–22.
 22. Ribeiro MBM, Freitas JV, Nogueira FGE, Farinas CS. Biosorption of Phenolic Compounds in Lignocellulosic Biomass Biorefineries. BioEnergy Res. 2020 Nov 16;
 23. Marbawi H, Khudri MAMRS, Othman AR, Halmi MIE, Gansau JA, Yasid NA, et al. Isothermal modelling of the adsorption of glyphosate onto palm oil fronds activated carbon. J Environ Microbiol Toxicol. 2019 Jul 31;7(1):21–6.
 24. Sha'arani SAW, Khudri MAMRS, Othman AR, Halmi MIE, Yasid NA, Shukor MY. Kinetic analysis of the adsorption of the brominated flame retardant 4-bromodiphenyl ether onto biochar-immobilized *Sphingomonas* sp. Bioremediation Sci Technol Res. 2019 Jul 31;7(1):8–12.
 25. Jaafar 'Izazy Nur Mohd, Sabullah K, Othman AR, Yasid NA, Halmi MIE, Shukor MY. Kinetics of the removal of polybrominated diphenyl ethers from aqueous solutions by using pressure steam-washed black tea. J Environ Microbiol Toxicol. 2019 Dec 31;7(2):26–31.
 26. Conrad EK, Nnaemeka OJ, Chris AO. Adsorptive Removal of Methylene Blue from Aqueous Solution Using Agricultural Waste: Equilibrium, Kinetic and Thermodynamic Studies. Am J Chem Mater Sci. 2015 Nov 4;2(3):14.
 27. Acemioğlu B. Adsorption of Congo red from aqueous solution onto calcium-rich fly ash. J Colloid Interface Sci. 2004 Jun 15;274(2):371–9.
 28. Onwuka GI. Food analysis and instrumentation: theory and practice. Nigeria: Naphathali prints; 2005.
 29. Datugun P. Adsorption Of Dyes On Sorghum Husk And Grounut Shell From Agricultural Wastes [BSc.]. [Bauchi, Nigeria.]: Abubakar Tafawa Balewa University; 2018.
 30. Patil S, Renukdas S, Patel N. Removal of methylene blue, a basic dye from aqueous solutions by adsorption using teak tree (*Tectona grandis*) bark powder. J Environ Sci. 2011;1(5):711–26.
 31. Folorunsho AT, Abel UA, Promise EU. A Statistical Approach to Optimization of Congo Red Dye Removal (CRDR) Via Coconut Shell Activated Carbon (CSAC). Int J Comput Theor Chem. 2016 Dec 22;4(2):7.
 32. Zhang J, Stanforth R. Slow Adsorption Reaction between Arsenic Species and Goethite (α -FeOOH): Diffusion or Heterogeneous Surface Reaction Control. Langmuir. 2005 Mar 1;21(7):2895–901.
 33. Bharathi KS, Ramesh ST. Removal of dyes using agricultural waste as low-cost adsorbents: a review. Appl Water Sci. 2013 Dec 1;3(4):773–90.
 34. Brunauer S, Emmett PH, Teller E. Adsorption of gases in multimolecular layers. J Am Chem Soc. 1938;60(2):309–19.
 35. Ismaila S. Application of Biowaste as low cost adsorbent for removal of Methylene Blue dye from aqueous solution [BSc.]. [Bauchi, Nigeria.]: Abubakar Tafawa Balewa University; 2017.
 36. Idan IJ, Abdullah LC, Choong TS, Jamil SNABM. Equilibrium, kinetics and thermodynamic adsorption studies of acid dyes on adsorbent developed from kenaf core fiber. Adsorpt Sci Technol. 2018 Feb 1;36(1–2):694–712.
 37. Hameed BH, Daud FBM. Adsorption studies of basic dye on activated carbon derived from agricultural waste: *Hevea brasiliensis* seed coat. Chem Eng J. 2008;139(1):48–55.